

---

## Antimicrobial, TG-DTA, X-ray Studies of Novel Zn(II), Cu(II), Ni(II) and Co(III) Metal Complexes Derived from 1-ethyl-3-acetyl-4-hydroxy-2(1H)-Quinolone Derivative

<sup>1</sup>Archana A. Kachare, Shankar <sup>1</sup>N. Ipper, <sup>2</sup>Pavan R. Kale, <sup>3\*</sup>Mahananda A. Raut

<sup>1</sup> Department of Chemistry, Sunderrao Solanke Mahavidyalaya, Majalgaon, (MS), 431131, India

<sup>2</sup>Rajarshi Shahu Arts, Commerce and Science College, Pathri, Phulambri, (MS), 431004, India

<sup>3\*</sup>Department of Chemistry, Pratishthan Mahavidyalaya, Paithan, (MS), 431107, India

Corresponding Author E-mail: [mahanandaraut@yahoo.com](mailto:mahanandaraut@yahoo.com)

### Abstract:

A Mononuclear octahedral complexes of Zn(II), Cu(II), Ni(II) and Co(III) has been derived from N<sub>2</sub>O donor Schiff base hydrazone ligand (*E*)-3-(1-(2-(benzo[d]thiazol-2yl)hydrazono)ethyl)-1-ethyl-4-hydroxyquinolin-2(1H)-one. The ligand and its complexes were characterized on the basis of elemental analysis, magnetic susceptibility, UV visible spectra, FTIR, <sup>1</sup>H NMR spectra, mass spectra, TG-DTA and XRD studies. The spectral study reveals that metal complex possess an octahedral geometry with 1:2 metals to ligand (ML<sub>2</sub>) stoichiometry. The X-ray study revealed that Ni (II) and Co (III) complexes are monoclinic with one atom per unit cell. The ligand and complexes have been screened for their antibacterial activity using the Agar cup method employing Penicillin as a standard drug microbial strains were used *Escherchia coli*, *Salmonalla typhi*, *Staphylococcus aureus* and *Bacillus substilis*. The antibacterial activity of ligand and its complex illustrates that the complexes shows higher activity than ligand. The ligand and its complexes show higher activity against *Staphylococcus aureus* and *Bacillus substill* Seems to than *Escherchia coli*, *Salmonalla typhi*. Antifungal activity of ligand and complexes were tested against *in vitro* against fungi that are *Aspergillus niger*, *Penicilum chrysoganum*, *Fusarium moniliforme* and *Aspergillus flavus* by poison plate method using potato dextrose agar medium at fixed (1%) concentration. Ligand does not show antifungal activity but complexes are showing better antifungal activity. Which suggest that the incorporation of metal in the ligand results in increasing the antimicrobial activity.

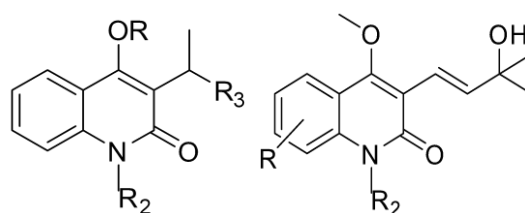
**Keywords:** Antimicrobial; TG-DTA; X-ray Studies; Metal Complexes; Quinolone Derivative;

### INTRODUCTION:

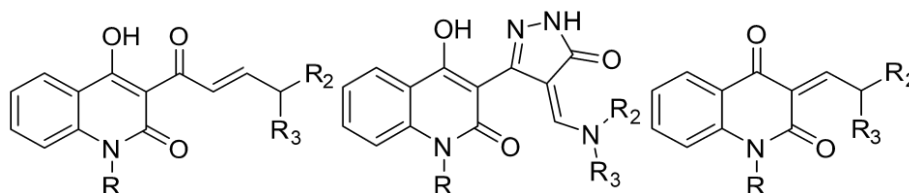
The continuous interest in transition metal complexes of 2-Quinolone derivatives attributed to many reasons. They have amazing potential of biological activities including were found to be associated with various biological activities such as antitumor [1,2], antiulcer [3], anti-inflammatory [4], antibacterial [5], antiplatelet [6], antioxidant [7] and antidepressant, antifungal, anticonvulsant and cardiac activity [8]. Many substituted

---

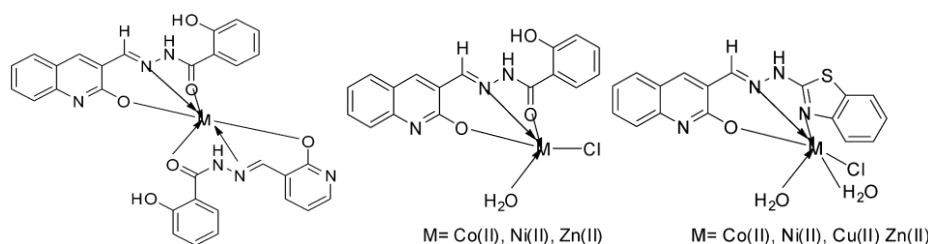
quinoline-2- one derivative have recently craned great interest in chemotherapy as antitumor drugs. Substituted 4- alkoxy and 4- hydroxy-quinoline-2(1*H*) - ones such as glucocitolones (**Figure a, b**) [9] are widely found among quinoline alkaloids of rutaceous plants[10] Compound glucocitlones also form a valuable class of biologically active molecules including human immunodeficiency virus type (HIV-1) integrase inhibitors[11] and hepatitis C virus (HCV) inhibitor [12]. Therefore diversity- oriented for the preparation this class of compounds in a practical and concise manner would be very useful for drug discovery.


**(Figure a, b)**

Enamlnones derived from 3-(un) substituted 4-hydroxy quinolin-2-(1*H*)-ones shows molluscicidal activities against *Biomphalaria alexandrina* and *Lymnaeae natalensis* snails. Many quinoline alkaloids and quinolinone derivatives were reported to exhibit important molluscicidal potency. eg. atanine, a quinolinone alkaloid, show potential activity against larvae [13]. Following be the structures of enamlnones (**Figure c, d, e**)


**(Figure c, d, e)**

Taking account of importance of 2-quinolone moiety many researchers used to synthesize Schiff base hydrazones of 2-quinolone. DNA binding studies of novel Co(II), Ni(II), Cu(II), and Zn(II) complexes of Schiff base ligands with quinoline core, studied by G. Kuredkar *et.al.*[14] Structure shown in (**Figure f, g, h**)


**(Figure f, g, h)**

Biologically active transition metal chelates of Ni(II), Cu(II) and Zn(II) of 2-Aminothiazole was synthesized by Z. Chohan *et al* [15] taking account the importance of Schiff base hydrazone complexes [16,17] we derived novel Zn(II), Cu(II), Ni(II) and Co(III) metal complexes of (*E*)-3-(1-(2-(benzo[*d*]thiazol-2yl)hydrazono)ethyl)-1-ethyl-4-hydroxyquinolin-2(*IH*)-one as a ligand.

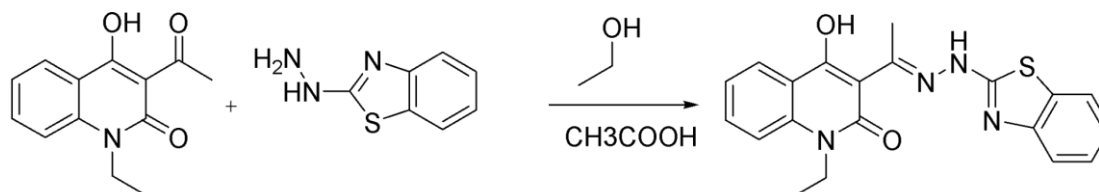
### **EXPERIMENTAL:**

All chemicals were of AR grade purchased from Sigma Aldrich and used for synthesis of ligand. For the synthesis of metal complexes AR grade metal nitrates of Cu (II), Ni (II), Zn (II) and Co (II) acetate were used from S. D. fine chemicals. Spectral grade solvents were used for spectral measurements. The carbon, hydrogen, nitrogen contents were determined on Perkin Elmer (2400) CHNS analyzer. IR spectra were recorded on a FT-IR Bruker spectrophotometer in 400-4000  $\text{cm}^{-1}$  range. The UV/ Vis spectra were recorded on Shimadzu UV 160 spectrophotometer for complex in DMSO.  $^1\text{H-NMR}$  spectra of ligand measured in DMSO using TMS as an internal standard. The LC- MS spectra were recorded on a Waters, Q-TOF Micro mass (LC-MS). Magnetic moments were measured by Guoy's method and were corrected for diamagnetism of the components using Pascal's constants. Conductance was measured on Elico Cm-180 Conducto meter using  $10^{-3}$  M solution in DMSO. Powder XRD studies were carried out with a Bruker AXS D8 Advance X-ray diffractometer.

### **Synthesis of ligand:**

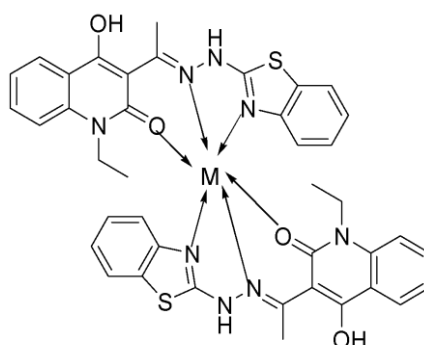
The starting material for our ligand synthesis was 3-Acetyl-1-ethyl-4-hydroxy-2(*IH*)-quinolone synthesized in laboratory according to known method Kappe *et al* [18]. 3-Acetyl-1-ethyl-4-hydroxy-2(*IH*)-quinolone (10.85 gm 0.05 mol) was taken in clean and dry round bottomed flask and 50 mL ethanol was added in it. The solution was warmed. To this, 5-10 mL of glacial acetic acid was added as a catalyst and (8.26 gm, 0.05 mol) of 2-hydrazino benzothiazole was added in it. This reaction mixture was refluxed and stirred for 1/2 hr. on rota heating mantel. Yellow solid product formed was filtered off, washed with ethanol and dried in vacuum desiccators.

The product was recrystallized from DMF-ethanol mixture (yield 85%) m. p. 241°C


**Scheme 1**

### Synthesis of metal complex:

To the hot solution of ligand in ethanol (0.02 mol in 25mL), hot ethanolic solution of metal nitrate salts (0.01 mol in 25 mL) was added drop wise. For the synthesis of cobalt complex salt of acetate was used. To this reaction mixture, 10% ethanolic ammonia was added to adjust the pH of solution to 7.5 to 8.5. The reaction mixture stirred for 3-5 hours in warm condition on magnetic stirrer to get complex in solid form. The solid complex was filtered off, washed several times with ethanol and dried in vacuum over  $\text{CaCl}_2$ .


**Scheme 2**

Above be the proposed structure of complexes Where  $M = \text{Cu (II)}, \text{Ni (II)}, \text{Zn (II)}$  and  $\text{Co (III)}$

### RESULTS AND DISCUSSION:

All complexes are coloured solids, stable for air and heat. The complexes are insoluble in water, ethanol, methanol, DCM but easily soluble in polar solvents DMF /DMSO. The analytical data indicate that ligand  $L = (E)\text{-3-(1-(2-(benzo[d]thiazol-2yl)hydrazono)ethyl)-1-ethyl-4-hydroxyquinolin-2(1H)-one}$  condensed with transition metal salt in 1:2metal to ligand molar ratio and the product formed well defined complexes can be symbolized as follows  $\text{ZnL}_2, \text{CuL}_2, \text{NiL}_2, \text{CoL}_2$ . Molar conductance measurements were measured in DMSO ( $10^{-3}\text{M}$ ) solutions at room temperature and are present in Table 1 The molar conductance data indicate that all complexes are non-electrolytic in nature. Magnetic

susceptibility of the powdered complexes were carried out by using Guoy's balance method at room temperature with  $\text{Hg}[\text{Co}(\text{SCN})_4]$  as a calibrant.

**Table 1:** Physical, Analytical Data of Ligand and its Metal Complexes:

Compound	Mol.formula	Color	M.P. °C	Mol. Wt.	C%	H%	N%	O%	S%	Metal %	$\mu_{\text{eff}}$ B.M.	Molar conductance $\text{Ohm}^{-1} \text{cm}^2 \text{mol}^{-1}$
HL	$[\text{C}_{20}\text{H}_{18}\text{N}_4\text{O}_2\text{S}]$	Yellow	241	378	63.10 (63.48)	4.34 (4.79)	15.18 (14.80)	8.91 (8.46)	8.47 (8.47)			---
$\text{ZnL}_2$	$[\text{C}_{40}\text{H}_{36}\text{N}_8\text{O}_4\text{S}_2\text{Zn}]$	yellow	>300	822	55.51 (55.12)	3.92 (4.01)	13.62 (13.73)	7.78 (8.21)	7.80 (7.94)	7.95 (8.13)	diamagnetic	11
$\text{CuL}_2$	$[\text{C}_{40}\text{H}_{36}\text{N}_8\text{O}_4\text{S}_2\text{Cu}]$	green	>250	820	55.94 (55.64)	4.21 (3.93)	13.85 (13.74)	7.13 (7.80)	7.73 (7.81)	7.42 (7.74)	1.75	3.1
$\text{NiL}_2$	$[\text{C}_{40}\text{H}_{36}\text{N}_8\text{O}_4\text{S}_2\text{Ni}]$	green	>300	811	56.17 (55.97)	4.01 (3.95)	14.54 (13.74)	7.91 (7.84)	8.17 (7.86)	7.85 (7.22)	diamagnetic	8.6
$\text{CoL}_2$	$[\text{C}_{40}\text{H}_{36}\text{N}_8\text{O}_4\text{S}_2\text{Co}]$	Dark brown	>300	816	60.14 (55.95)	3.85 (3.95)	13.47 (13.78)	7.49 (7.84)	7.89 (7.34)	7.59 (7.22)	diamagnetic	7.7

### Electronic absorption spectra:

The electronic absorption spectra of ligand and its complexes were recorded in DMSO over the range 200-800 nm shown in **Figure 1**. The electronic spectrum of ligand shown in **Figure 1(a)** which exhibits three absorption bands at 247.50 nm, and 287.5 nm and 367.5 nm assigned to the  $n-\pi^*$  and  $\pi-\pi^*$  transitions of hydroxy, azomethine and 2-quinolone carbonyl respectively [19]. These bands are present in complexes but in blue shift. The type of d-d transitions cannot be identified due to colour dominance of charge transfer band in complexes. The Cu (II) complex has a magnetic moment 1.75 BM indicating the presence of one unpaired electrons [20]. **Figure 1(b)** of Cu (II) shows UV transition band in the range  $25031 \text{ cm}^{-1}$  (399.5 nm) attributed to  ${}^2\text{B}_{1g} \rightarrow {}^2\text{E}_g$  and charge transfer band observed at  $38610 \text{ cm}^{-1}$  (259 nm) indicating distorted octahedral geometry around the Cu (II) ion [21]. Zn (II), Ni (II) complexes are diamagnetic indicating  $d^8$ ,  $d^{10}$  octahedral geometry [22, 23]. In the electronic spectra of the Ni(II) **Figure 1(c)** complex show d-d band at  $26385 \text{ cm}^{-1}$  (379 nm) assigned to the diamagnetic  ${}^3\text{A}_{2g} \rightarrow {}^3\text{T}_{1g}$  (P) spin allowed transition, consistent with their pseudo-octahedral configuration also shows charge transfer band at  $30675 \text{ cm}^{-1}$  (326 nm) [24]. The diamagnetic Zn (II) complex shown in **Figure (d)**, did not show d-d band and its

spectrum is dominated only by a charge transfer. We used Co (II) acetate but due to air oxidation Co (III) complex was formed and that is diamagnetic it from low spin octahedral geometry [25, 26]. The electronic spectrum of synthesized complexes exhibits low energy absorption. The Co (III) complex shows a diamagnetic character. The electronic spectrum of this **Figure 1(e)**, complex is also consistent with its octahedral environment around the Co (III) ion. The spectra display two bands at  $23256\text{ cm}^{-1}$  (429 nm),  $28248\text{ cm}^{-1}$  (354 nm) due to  ${}^6A_{1g} \rightarrow {}^1T_{2g}$ , charge transfer band respectively [27].

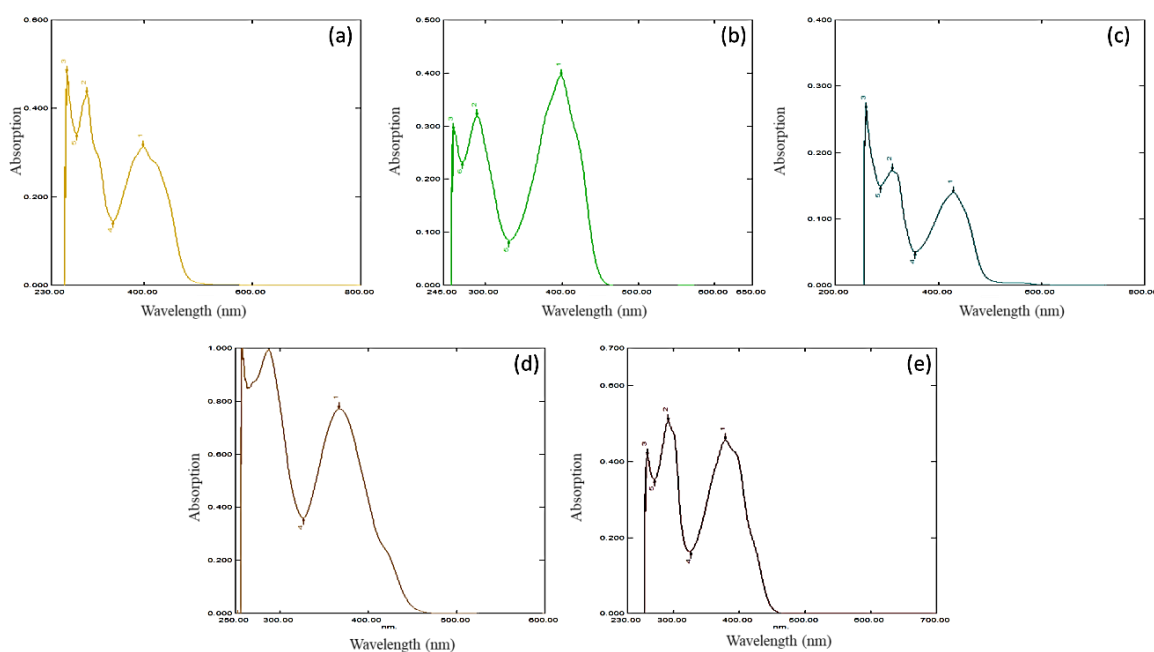


**Figure 1:** UV. Spectrums of (a) ligand, (b)  $\text{CuL}_2$ , (c)  $\text{NiL}_2$ , (d)  $\text{ZnL}_2$ , (e)  $\text{CoL}_2$  complexes

#### FTIR spectra:

The FT-IR spectrum of metal complexes shown in **Figure 2** was compared with that of free ligand in order to investigate the mode of chelation of metal ions with ligand. In the FT-IR spectrum in **Figure 2(a)** for free ligand shows some characteristic bands at  $3398$ ,  $3109$ ,  $1654$ ,  $1594$ ,  $1556$ ,  $742\text{ cm}^{-1}$  assigned to enolic -OH, NH, C=O (quinolone),  $>\text{C}=\text{N}$  (azomethine),  $>\text{C}=\text{N}$  (ring), N-H out of plane stretching, respectively [28]. In both complexes the ligand behaves as ONN tridentate via the  $>\text{C}=\text{O}$  (quinolone),  $>\text{C}=\text{N}$  (azomethine) and  $>\text{C}=\text{N}$  (in benzothiazole ring) groups. This fact is supported by the following evidences. **Figure 2(b)** and **Figure 2(c)** represents the IR spectra of complexes. There is presence of a band in the region  $3307\text{--}3398\text{ cm}^{-1}$  due to OH indicating 4-hydroxy group of quinolone does not take part in coordination. The IR stretching frequency of  $>\text{C}=\text{O}$  (quinolone) in the

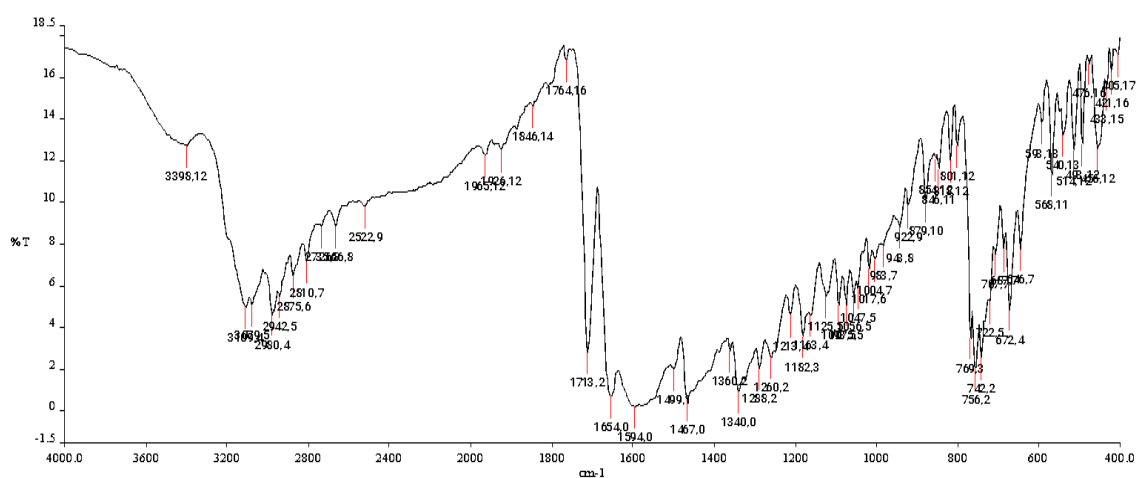
(An open access scholarly, peer-reviewed, interdisciplinary, monthly, and fully refereed journal.)

complexes observed in the region  $1592\text{-}1609\text{ cm}^{-1}$  in complexes. This Shift to lower frequency of carbonyl group of quinolone by  $45\text{-}62\text{ cm}^{-1}$  indicate the coordination of  $>\text{C}=\text{O}$  to metal ion. The shift of azomethine  $>\text{C}=\text{N}$  group to lower frequency region by  $22\text{-}05\text{ cm}^{-1}$  with respect to free ligand, indicates that the nitrogen of the azomethine group coordinate to the metal ion. It was further supported by upward shift in  $-\text{N-H}$  out of plane bending in complexes. The  $>\text{C}=\text{N}$  (benzothiazole ring) groups shift to lower frequency which indicates that they form coordinate bond with metal atom. TSalient features of IR spectral data of ligand and complexes has given in **Table 2**. The FT-IR stretching frequency of  $>\text{C}=\text{O}$  (quinolone),  $>\text{C}=\text{N}$  (azomethine),  $>\text{C}=\text{N}$  (benzothiazole ring) groups shift to lower frequency range which indicates that they form coordinate bond with metal atom [29].

**Table 2: Salient Features of IR Spectral Data of Ligands.**

(Assignment of band frequencies to bond vibration modes)

Ligands	$\nu(\text{OH})$ Enolic	$\nu(\text{NH})$ Hydrazone	$\nu(\text{C}=\text{O})$ Quinolone	$\nu(\text{C}=\text{N})$ Azomethine	$\nu(\text{C}=\text{N})$ Ring nitrogen	$\nu$ ( $\text{C}=\text{C}$ )	$\nu(-\text{NH})$ out of plane
Ligand	3398 (b)	3109 (b)	1654 (s)	1594 (b)	1556	1467 (s)	742 (s)
ZnL <sub>2</sub>	3222	-	1631	1598	1536	1415	753
CuL <sub>2</sub>	3307 (m)	3212 (s)	1592 (s)	1572 (s)	1545 (s)	1411 (s)	738 (s)
NiL <sub>2</sub>	3398	3119	1595	1572	1532	1409	753
CoL <sub>2</sub>	3351 (b)	3057 (b)	-	1591 (s)	1543 (s)	1420 (s)	753 (s)



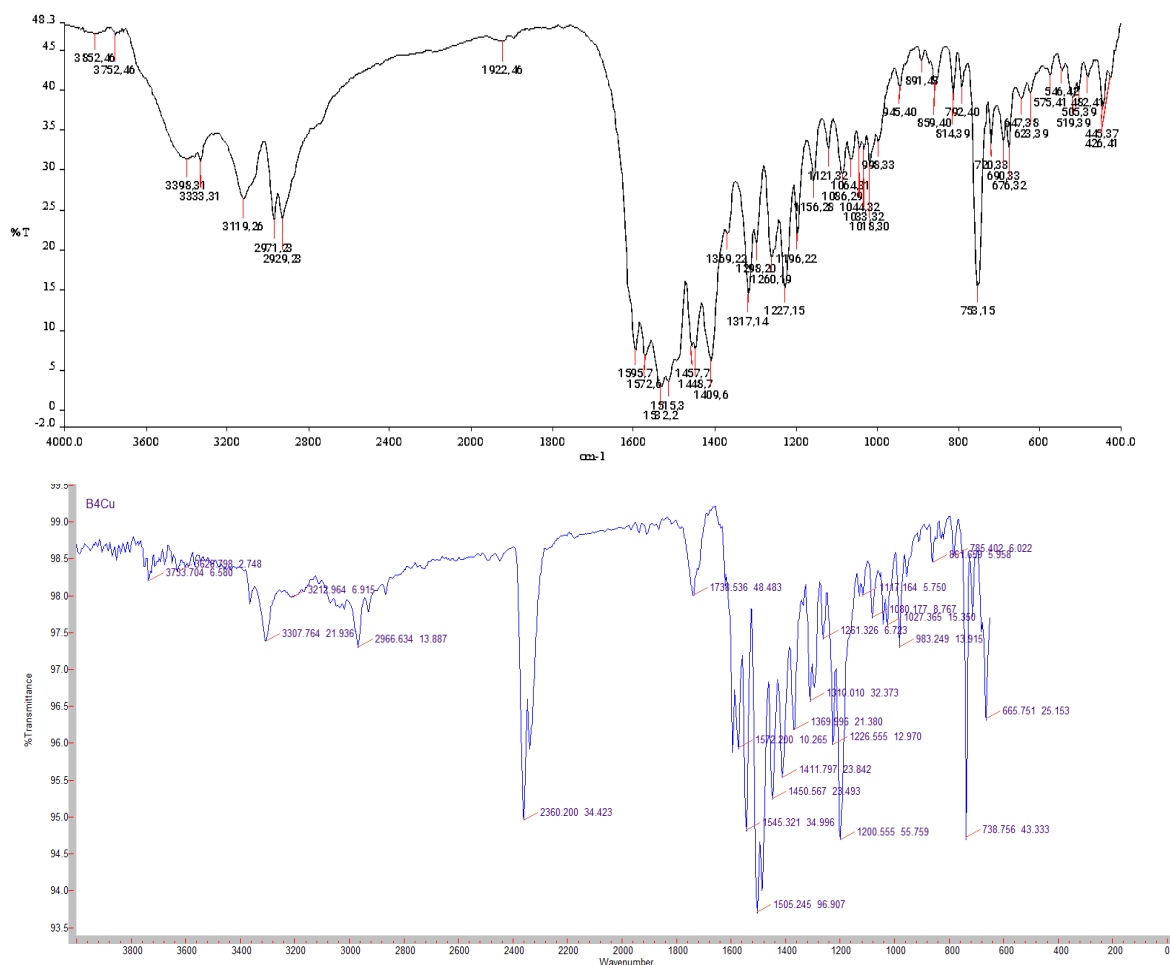


**Figure 2:** FT-IR Spectrums of (a) ligand, (b) NiL<sub>2</sub> and (c) CuL<sub>2</sub>

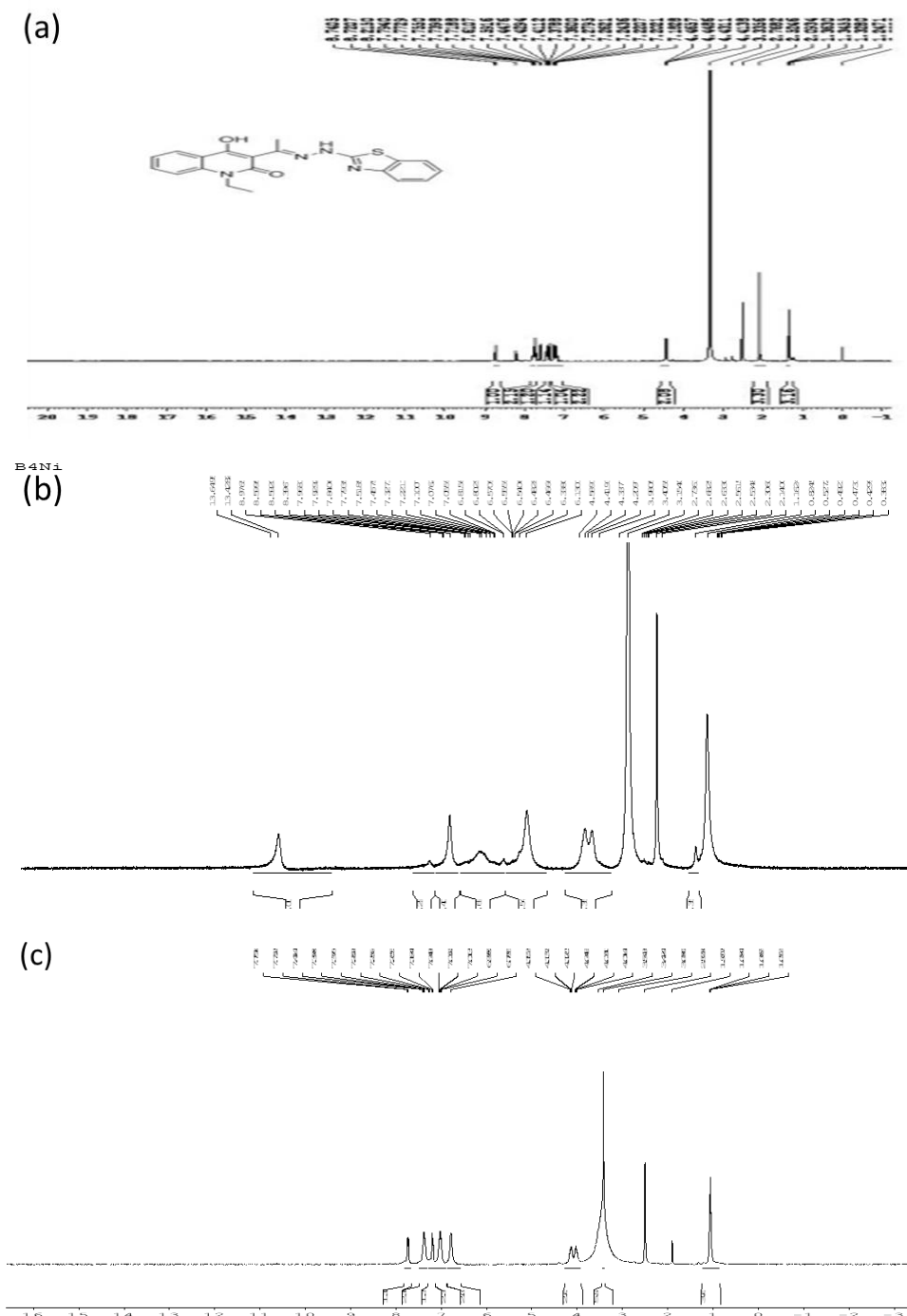
### <sup>1</sup>H-NMR Spectral Studies:

<sup>1</sup>H NMR Spectra of ligand was recorded in DMSO and shown in **Figure 3(a)**. It shows signals at 1.34 (t, 3H, N-CH<sub>2</sub>-CH<sub>3</sub><sup>\*</sup>), 2.76 ppm. (s, 3H, N=C-CH<sub>3</sub>), 4.44 ppm. (s, 2H, N-CH<sub>2</sub>), 7.18-8.21 ppm. (m, 8H, H<sub>arom</sub>), 11.98 ppm. (s, 1H, N-H), 16.81 □ (s, 1H, OH<sub>enolic</sub>) [30]. The formation of metal complex is confirmed by <sup>1</sup>H NMR spectral study of **Figure 3(b)** for the Ni (II) and **Figure 3(c)** Co (III) complexes. The <sup>1</sup>H NMR spectra of ligand show chemical shift at 16.80 δ ppm assigned to enolic proton of 4-hydroxy-quinolone. The appearance of this chemical shift in the complex at 13.64 δ ppm. That indicate non coordination of enolic -OH. The upfield shift in the δ chemical shift of -OH may be due to the change in environment of enolic -OH group. The value of -NH proton in the ligand appear at 11.98 δ ppm [31]. But in complex the δ chemical shift for -NH proton appears at 8.91 δ ppm in the up field region evidence for the coordination of adjacent C=N of hydrazone to metal ion. The azomethine -



(An open access scholarly, peer-reviewed, interdisciplinary, monthly, and fully refereed journal.)

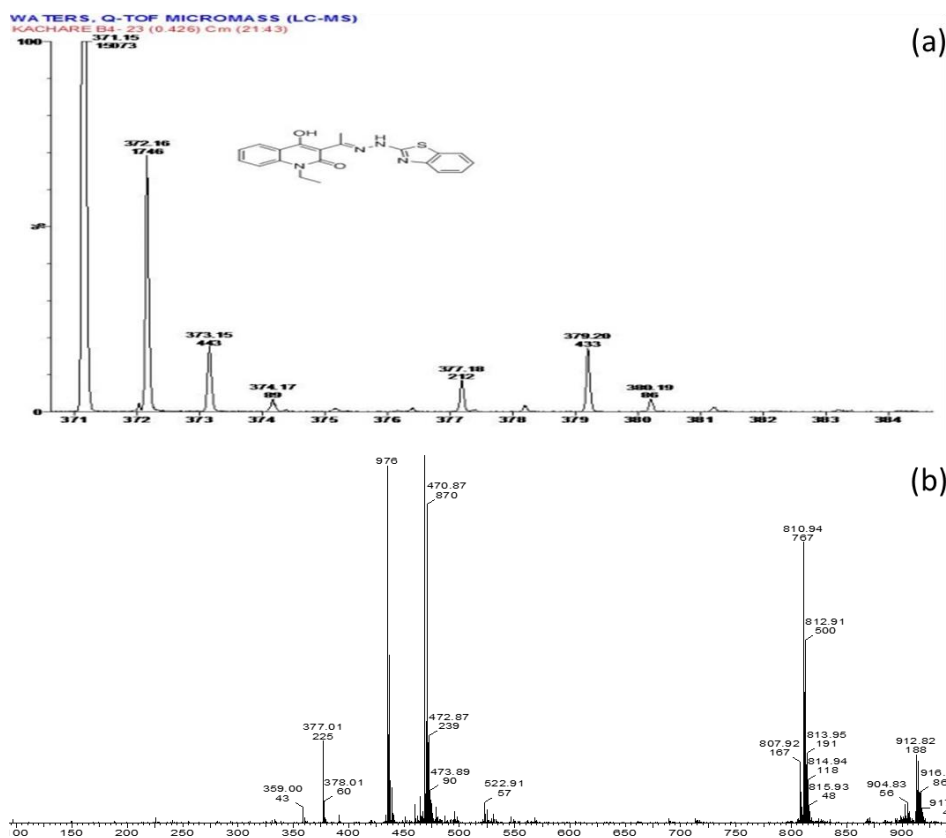
CH<sub>3</sub> proton having  $\delta$  chemical shift at 2.75  $\delta$  ppm in the ligand appear in at 2.35  $\delta$  ppm in the complex. This up field shift indicates coordination of azomethine nitrogen to the metal ion.



**Figure 3:** <sup>1</sup>H-NMR Spectra of (a) Ligand, (b) NiL<sub>2</sub> (c) CoL<sub>2</sub> complex

**Mass spectra of ligand and complexes:**

In the **Figure 4** shows the mass spectrum of ligand and complexes supports there proposed formulation. The molecular ion peak of the ligand shown in **Figure 4(a)** was observed at  $m/z$  380.19 ( $M+2$ ), 379.20 ( $M+1$ ),  $m/z$  at 378.1 a.m.u. which is equal to calculated mass from the proposed structure. The mass spectrums of representative metal complexes Ni (II), and Co (III) given in **Figure 4(b)** and **Figure 4(c)**. The molecular ion peak [ $M^+$ ] of Ni (II), Co (III) complexes are observed at,  $m/z$  815.93, 814.91 respectively corresponding to their molecular masses. The fragmentation peak in metal complexes indicates loss of two enolic hydrogens of hydroxyl groups forms base peaks [32]. The masses of ligand and complexes exactly match with their calculated masses.



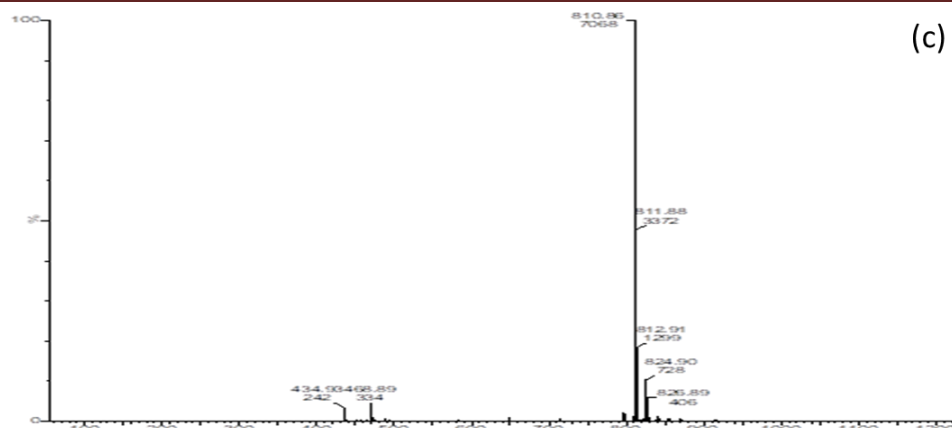


**Figure 4: Mass spectra of (a) ligand, (b) Ni L<sub>2</sub> and (c) Co L<sub>2</sub> complex**

### Thermo-gravimetric Studies:

The simultaneous TG/DT analysis of a representative Ni (II), Co (III) complex were studied and shown in **Figure 5**. The thermogram of Ni (II) complex of **Figure 5(a)** shows high thermal stability and two step decomposition. The first step within temperature range 230-530 °C with mass loss of 58.84 % (calculated weight loss 59.10 %) due to loss of non-coordinated part of ligand. This is confirmed by endothermic peak at 326.10 °C in DTA curve. The second step decomposition observed within 560-800 °C with weight loss of 28 %. This may be due to loss of coordinated part of metal complex. Beyond that TG curve attains a constant level corresponding to their metal oxide that is NiO [33].

The TG curve of Co (III) complex given in **Figure 5(b)** was the high thermal stability with curve shows three step decomposition. In the first two steps loss of non-coordinated part of ligand takes place. In the first step weight loss of 25.85 % (calculated weight loss 26.48 %) up to 380 °C may be due to loss of two C<sub>6</sub>H<sub>4</sub>S fragment, which is supported by endothermic peak at 309.83 °C. The second stage decomposition occurs with mass loss of 28.83 % (calc. wt. loss 29.17 %) in the range 380-530 °C, due to loss of two *N*-ethyl aniline fragments. This is authenticated by broad endotherm in DTA curve. In third step of decomposition with weight loss of 37 % within temperature 540-800 °C, corresponds to decomposition of coordinated part of complex. Above 800 °C, the TG curve attains a constant level corresponding to their metal oxide [34].

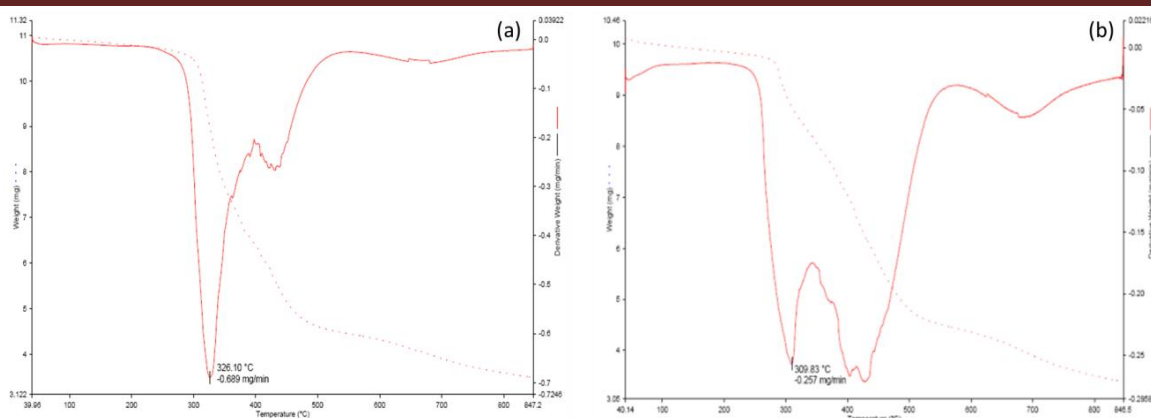


**Figure 5:** TG curve of (a) Ni (II) and (b) Co (III) complex

The thermal kinetic parameters  $\Delta S$ ,  $E_a$  and  $Z$  for non- isothermal decomposition of complexes have been calculated by Coats-Redfern method [35] by using TG-DTA curves of presented in **Table 3**. Generally, with decreasing value of  $\Delta E$ , the value of  $Z$  increases, and higher value of activation energy suggest higher stability [36]. In the present complexes, the value of  $E_a$  decrease with the increasing value of ( $Z$ ) i.e. frequency factor indicating that the activated complexes have more ordered or more rigid structure than the reactants or intermediate and that the reactions are slower than normal.

**Table 3:** Thermodynamic and Kinetic Parameters

Metal complex	Method	Step	Decomp. Temp.	Order of Reaction	$E_a$ (KJ mol <sup>-1</sup> )	$\Delta S$ (KJ mol <sup>-1</sup> )	$\Delta G$ (KJ mol <sup>-1</sup> )	$Z$ (S <sup>-1</sup> )	Correlation Coefficient (r)
NiL <sub>2</sub>	H-M C-R	I	440	0.55	23.04	-144.2	33.84	378993.4	0.9999
				0.55	15.97	-123.4	32.28	4640060.8	0.9989
	H-M C-R	II	847	0.55	3.23	-179	31.32	10785	0.9999
				0.55	10.23	-185.6	32.20	5474.0	0.9999
CoL <sub>2</sub>	H-M C-R	I	500	0.55	14.86	-149.31	26.05	206680.74	0.9969
				0.55	10.19	-142.19	25.51	486484.51	0.9919
	H-M C-R	II	800	0.55	12.90	-167.87	39.11	46227.81	0.9989
				0.55	11.69	-165.50	38.74	61484	0.999

**X-ray Diffraction Study:**

The X-ray diffractogram of metal complex were shown in **Figure 6**. It was scanned in between the range  $2\theta$  (°) of 0-60 at wavelength 1.54 Å. The diffractogram and associated data depict the  $2\theta$  (°) values for each peak, relative intensity and inter planer spacing (d-values). The diffractogram of Ni (II) complex had seventeen reflections shown in **Figure 6(a)** with maxima at  $2\theta$  (°) =10.73 corresponding to d value 8.23 Å having 110 hkl plane. The diffractogram of Co (III) complex had five reflections present in the **Figure 6(b)** maxima at  $2\theta$  (°) =10.067 corresponding to d value 8.788 Å. The X-ray diffraction pattern of the

complex with respect to major peaks having relative intensity greater than 10% have been indexed by using computer program [37]. The above indexing program gives hkl planes, unit cell parameters and volume of the unit cell. The unit cell of Ni (II) complex yielded values of lattice constants the standard deviation observed for NiL<sub>2</sub> is 0.20 % which is within the permissible limit of 2 %. The observed and calculated densities were 0.8634 gcm<sup>-3</sup> and 0.8513 gcm<sup>-3</sup> respectively. The volume is found to be 1589.90 Å<sup>3</sup> and complex crystallizes in the monoclinic system with 1 atom per unit cell [38,]. The lattice parameters are a = 21.395, b= 9.0 and c= 8.76 Å, α = 90, β= 109.6125 and γ=90°. The unit cell of Co (III) complex yielded values of a = 21.39, b=8.98 and, c= 8.766 Å, α = γ 90°, β = 108.5°, V = 1616.26 Å<sup>3</sup>. In occurrence with these cell parameter, the condition such as a≠b≠c, α=γ=90°, β≠90° indicate both Ni (II) and Co (III) complexes has monoclinic crystal system [39, 40]. The indexed X-ray Diffraction data of representative Ni (II) Complex were shown in **Table 4**.

**Table 4:** Indexed X-ray Diffraction Data of Ni (II) Complex

Peak No.	2θ (observed)	2θ (calculated)	d (observed)	d (calculated)	Miller indices of Planes			Relative intensities (%)
					h	k	l	
1	8.901	8.768	9.92679	10.07687	-2	0	0	74.02
2	9.695	9.820	9.1156	9.00000	0	1	0	37.53
3	10.738	10.757	8.23264	8.21781	1	1	0	100
4	13.016	12.868	6.79602	6.87385	1	0	1	33.81
5	14.530	14.547	6.09138	6.08427	0	1	1	25.49
6	15.930	15.985	5.55888	5.53982	2	0	1	5.26
7	17.186	17.255	5.15546	5.13508	-4	0	1	22.90
8	20.041	20.182	4.42705	4.39639	-4	1	0	46.66
9	20.582	20.442	4.31185	4.34104	-1	0	2	72.13
10	21.49	21.507	4.13147	4.12843	0	0	2	10.11
11	22.183	22.202	4.00215	4.00069	-1	2	1	6.97
12	25.056	25.023	3.55112	3.55570	-6	0	1	22.68
13	25.721	25.572	3.4675	3.48066	4	1	1	55.84
14	26.913	26.939	3.31011	3.30697	-6	1	1	10.92
15	27.662	27.673	3.22227	3.22097	5	0	1	10.9
16	29.563	29.429	3.01923	3.03261	5	1	1	8.15
17	30.327	30.308	2.94487	2.94662	-4	2	2	5.36

#### Unit cell data and crystal lattice parameters

a (Å) = 21.395, b (Å) = 9.0, c (Å) = 8.7654; α = 90°, β = 109.612°, γ = 90°; Z = 1; Volume (V) = 1589.9 Å<sup>3</sup>, Density (obs.) = 0.8634 gcm<sup>-3</sup>, Density (cal.) = 0.8513 gcm<sup>-3</sup>; Crystal system = Monoclinic, Space group = P2/m, Standard deviation (%) = 0.20

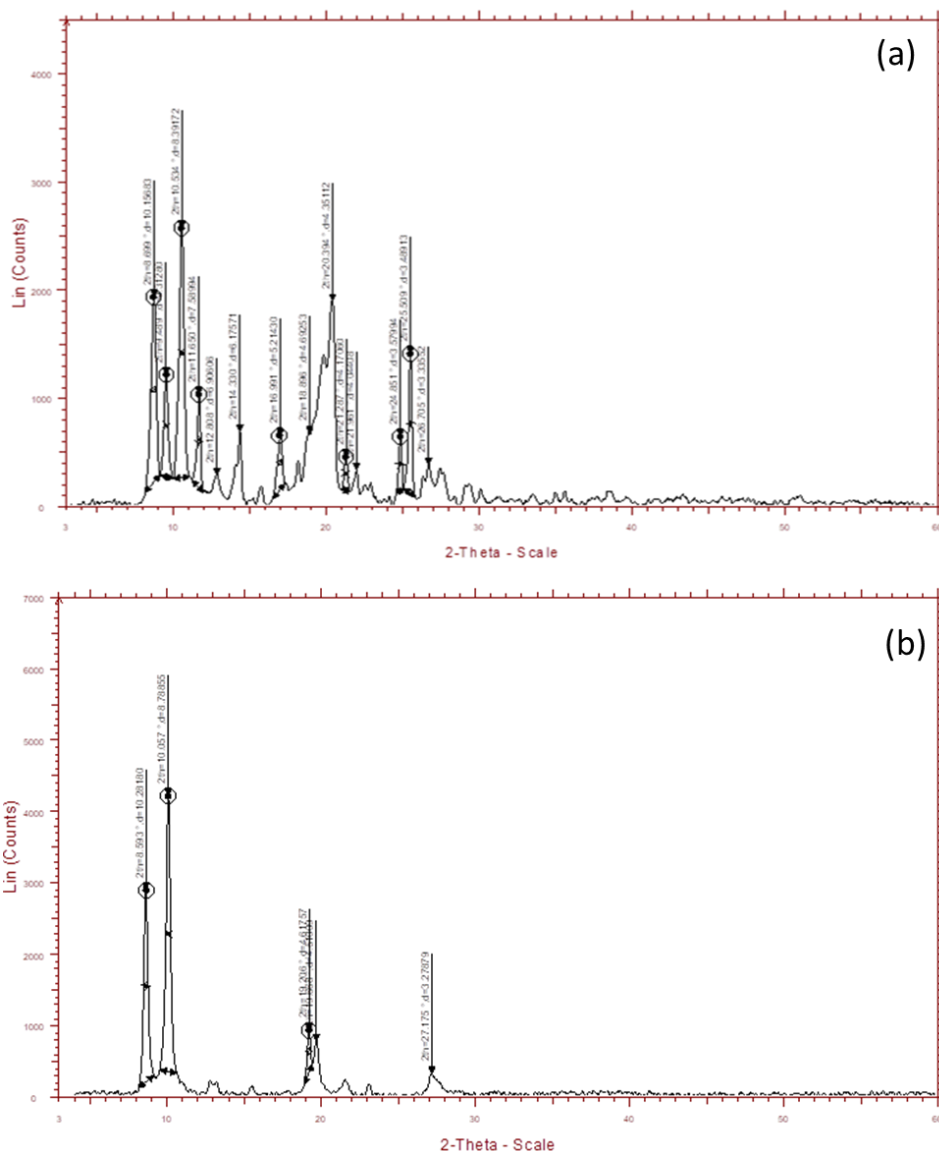


Figure 17. X-ray diffractogram of Ni(II) complex of ligand

**Biological activity of the compounds:**

***In vitro* antibacterial activity of the compounds:**

The antimicrobial activity of the ligand and the complex were tested against the standard microbial strains, *Escherishia coli*, *Salmonella typhi*, *staphylococcus aureus*, *Bacillus subtilis* by agar cup method [41] at fixed concentration of 1% in DMSO. The test was performed on nutrient agar Cup of 10 mm diameter were bored in the agar plate with sterile cork borer. All solutions were prepared in DMSO (1%) was added to cup, One cup for DMSO as blank and other for standard reference Penicillium was also placed on the seeded nutrient agar. Then the plates were shifted to incubator at 37 °C and incubated for 24 hours. The

activity was measured in diameter (mm). The results obtained are presented in **Table 5**. Inspection of the data revealed that both complexes and ligand show low activity towards Gram-negative bacteria *E. coli* and *S. typhi*. On the other hand, ligand and complexes shows activity against Gram-positive bacteria *S. aureus* and *B. substilius* [42, 43]. The activity of Cu (II), Ni (II) complexes shows highest antibacterial activity than other Zn (II) and Co (III) complexes [42]

**Table 5: Report for antibacterial testing.**

Medium - Nutrient Agar

Method- Agar cup method

Dose of compound - 1%

cup size - 10 mm

compound	<i>Escherishia coli</i>	<i>Salmonella typhi</i>	<i>Stapylococcus aureus</i>	<i>Bacillus subtilis</i>
Ligand(L)	8	11	14	16
(ZnL <sub>2</sub> )	13	15	15	15
(CuL <sub>2</sub> )	19	23	22	20
(NiL <sub>2</sub> )	25	28	21	27
(CoL <sub>2</sub> )	9	10	10	13
Penicillin	28	36	14	20

**Legends:** -ve = No Antibacterial Activity; Zone of inhibition = --- mm

***In vitro* antifungal activity of the compounds:**

Compound were screened in vitro against *Aspergillus niger*, *Penicilium chrysogenum*, *fusarium moneliforme*, *Aspergillus flavus*, by poison plate method with potato dextrose agar media. The compound were tested at the 1% concentration in DMSO and compared with control. Gresiofulvin was prepared as standard reference plate. The fungal suspension was spot inoculated on the plate's prepared using compound with nicrome wire loop. The plates were incubated at room temperature for 48 hours [44]. The result obtained is presented in **Table. 6**. The ligand does not show antifungal activity but its complexes shows appreciable activity. Antifungal activity of complexes increased several times on being coordinated with metal ions [45]. Zn (II), Cu (II) complexes shows more than 90% reduction of fungal growth for all fungi.

**Table 6:** Report for antibacterial testing.

Ligands	Antifungal growth			
	<i>Aspergillus niger</i>	<i>Aspergillus Flavus</i>	<i>Fusarium moniliforme</i>	<i>Penicillium chrysogenum</i>
	1%	1%	1%	1%
L	-ve	-ve	-ve	-ve
(ZnL <sub>2</sub> )	-ve	-ve	-ve	-ve
(CuL <sub>2</sub> )	-ve	-ve	-ve	-ve
(NiL <sub>2</sub> )	RG	+ve	-ve	-ve
(CoL <sub>2</sub> )	RG	-ve	RG	+ve
+ve control (DMSO)	+ve	+ve	+ve	+ve
-ve control (Griseofulvin)	-ve	-ve	-ve	-ve

Legends: + ve - Growth -(Antifungal Activity absent); -ve - No growth (More than 90 % reduction in growth Antifungal activity present); RG - Reduced Growth. (More than 50% reduction in growth observed)

**Conclusion:**

In the light of above discussion we have proposed octahedral geometry for all complexes. On the basis of physicochemical and spectral data discussed above, one can assume that the ligand behaves as, ONN tridentate, coordinating via quinolone carbonyl, azomethine nitrogen and nitrogen of benzothiazole ring in both complexes. The mass spectra of ligand and its metal complexes are in great accordance with calculated and observed. Thermogravimetric studies revealed that complexes are rigid and stable. The XRD study suggests monoclinic lattice type for Ni (II) and Co (III) complex. The complexes are more biologically active than free ligand.

**ACKNOWLEDGEMENTS**

The authors are thankful to the Head of Department, Dr. B. A. M. University, Chatrapati Sambhajinagar, for proving necessary facilities to perform this work.



---

**REFERENCES**

1. B. Joseph, F. Darro, A. Behard, B. Lesur, A. Frydman, R. Kiss, *J. Med. Chem.*, **45**, 2534-2555 (2002).
2. N. S. Rudrax, S. Shingade, M. Palkar, S. Deasai, *Current drug discovery technology* Volume **17** Issue **2**, [203 - 212] (2020); doi: [10.2174/1570163815666181008151037](https://doi.org/10.2174/1570163815666181008151037)
3. V. Ukarihets, A. Davidenko V, Gorkhova, *Chem. Heterocycl. comp.*, **46**, 974-986 (2012).
4. M. Ochid, F. Tabusa, M. Komatsu, T. Kanbe, K. Nakagawa, *Chem. Pharma. Bull.*, (Tokyo), **35**, 853-856 (1987).
5. J. Mikki, S.P. Baker, K.M. Standifer, T. Ishizel, Y. Chinda, J-W. Kusiak, *J. Med. Chem.* **30**, 1563-1566 (1987).
6. S. Jain, V. Chandra, P. Kumar Jain, K. Pathak, D. Pathak, A. Vaidya, *Arabian J. Chem.*, Vol **12** pp. 4920-4946, (2019); doi :[10.1016/j.arabjc.2016.10.009](https://doi.org/10.1016/j.arabjc.2016.10.009)
7. Moaz M. Abdou *Arabian Journal of Chemistry* Vol. **10** page 3324- 3337 (2017); <https://doi.org/10.1016/j.arabjc.2014.01.012>
8. O. Afzal, S. Kumar, M. Haider, R. Ali, M.R. Kumar, M. Jaggi, S. Bawa., *Eur J. Med. Chem.*, **97**, 871-910 (2015).
9. M. Sechi, C. Rizzi, A. Bacchi, M. Carcelli, D. Rogolino, N. Pala, T.W. Sanchez, L. Taheri, R. Dayam, N. Weamati, *Bioorganic Med. Chem.*, **17**, 2925-2935 (2009).
10. C. Melagraki, A. Afantis, H. Sarimveis, P.A. Koutentis, J. Markopoulos, *Bioorganic Med. Chem.*, **15**, 7237-7247 (2007).
11. Yusuke Kobiyashi, Takashitiharayama, *Tetrahedron Letters*. **50**, 6665-6567 (2009)
12. M. Abass, B.B. Mostafa, *Bioorganic and medicinal Chemistry*, **13**, **61**, 336144 (2005).
13. G. Wen-Tao, H. Wen-Duan, R. Mei, T. Li-Jun, *Synthetic Communications*, **40**, 732-738 (2010).
14. G. Kuredkar, S.M. Puttanagouda, S. Kulkarni, S. Budagumpi, V. Revankar, *Med. Chem. Res.*, **20**, 421-429 (2011).
15. Z.H. Chohan, *Met.-Based Drugs* **6**, 3 (1999)
16. S. Ihsan, A. Luay, S. Majed, A. Eveen, Y. Eyad, O. Rouzi, Mohammad, *Letters in Organic Chemistry*, **16**, 5, 430-436(7) (2019); <https://doi.org/10.2174/1570178616666181227122326>
17. M. Sunjuk, L. Al-najjar, M. Shatawi, B. Ei-Eswed, K. Sweidan, P. Bernhard, H. Zalloum, L. Ai-Essal, *inorganics*, **11** (10), 412; <https://doi.org/10.3390/inorganics11100412>

18. T.Kappe, R.Algner, M.Jobstil, P.Hohengassner, W. Stadelbauer, *Heterocyclic Communcation*,**1**, No. 5-6 (1993).
19. S. Elsayed, I. Buter, B. Claude, *Transition Met. Chem.*, **40**,179-187 (2015)
20. H. Althobiti, S. Zabin, *Open Chem.*, **18**, 591–607 (2020)
21. Y.Nishida, S. Kida, *Inorg. Nucl. Chem. Lett.* **7**, 325–328 (1971).
22. A.. El-Agamy, A. Abo-Attaia, *Arch. Appl. Sci. Res.*, **4**, 1139-1344 (2012)
23. Chohan, H.Z., *Synth. React, Inorg. Met. Org. Chem.*,**31**, (2001).
24. R.M. Ahmad, T.A. Hamdan, A.T. Numan,M.J Al-Jeboori, H. Potgieter, *Complex. Met.*, **1**, 38-45 (2014)
25. M. Das, S.Chattopadhyay,*Polyhedron***50**, 443-454 (2013).
26. S. Chattopadhaya, GBocelli,A. Musati, A.Ghosh, *Inorg. Chem. Commun.*,**9**, 1053 (2006).
27. STan, A. Al-Abbasi, M.I.M. Tahir, M.B. Kassim, *Polyhedron*,**68**, 287-294 (2014).
28. T. Kappe, R. Algner, M. Jobstil, P. Hohengassner, and W. Stadelbauer,*Prtl.Chem.*, Nos. **41**, 5-6 (1995).
29. P. Dapporto, M. Formica, V. Fusi, L. Giorgi, M. Micheloni, P. Paoli, R. Pontellini and P. Rossi, *Inorg. Chem.*, **40**, 6186 (2001); <https://doi.org/10.1021/ic0105415>.
30. A. El-Agamy, A.. Abo-Attaia,*Arch. Appl. Sci. Res.*, **4**,1139-1344 (2012)
31. E. Gungar, *Spectrochimica Acta Part A*, **314**, 216-221 (2012).
32. S. Elsayed, I. S. Butler, B.Claude, S. Mostafa, *Transition Met. Chem.*, **40**, 179-187 (2015).
33. , H-Q, Chang, L. Jia, J. Xu, W-N. Wu, T-F. Zhu,R-H., T-L. Ma, Y. Wang, Z-qXu, *Transition Met. Chem*,(2015).
34. M. Das, S. Chattopadnyay, *Polyhedron*, **50**, 443-451 (2013).
35. Coats, A., Redfern, J.P., *Nature*, 201, **68**,(1964).
36. Frost, A.A., Pearson, R.G., "*Kinetics and Mechanism*", John Wiley, New York (1961).
37. J. V. Carvajal, T. Roisnel, A. Winpoter, Grapnic tool For powder iffraction Laboratoris leon brillown (ced/ eners ) 91191 gif suryvette cedex. france (2004).
38. A. Datta, N. Chuang, J. Hung, *J. Chem Crystallography*, **41**, 1780-1784 (2011).
39. Datta, A., Chuang, N-T., Hung, J-H., *J. Chem Crystallography*, **41**, 1780-1784 (2011)
40. Nagwa Nawar and Nassir M. Hosny *Tran. Met. Chem.*, **25**, 1-8(2008).
41. Cruickshank R. J., Duguid P., Swain R. R., Publisher Churchill Lilingstone, *Medica Microbiology* **1**, (1998).
42. M. Angelusiu, S. Barbuceanu, C. Draghici, G. Almajan, *Eur. J. Med. Chem.*, **45**, 2055–2062 (2010).



43. J. Parekh, P. Inamdhar, R. Nair, S. Baluja and S. Chanda, *J. Serb. Chem. Soc.*, **70**, 1155 (2005); <https://doi.org/10.2298/JSC0510155P>
44. Y. Vaghasiya, R. Nair, M. Soni, S. Baluja and S. Shanda, *J. Serb. Chem. Soc.*, **69**, 991 (2004); <https://doi.org/10.2298/JSC0412991V>
45. N. Ingarsal, G. Saravanan, P. Amutha, S. Nagarajan, *EuropeanJournal of Medicinal Chemistry***42** (4), 517-520 (2007).